Chemistry & Biology
Article

A Conformationally Restricted Guanosine Analog Reveals the Catalytic Relevance of Three Structures of an RNA Enzyme

Rieko Yajima,[1] David J. Proctor,[2,4] Ryszard Kierzek,[3] Elzbieta Kierzek,[3] and Philip C. Bevilacqua[1,2,*]
[1] Huck Institute for the Life Sciences
[2] Department of Chemistry
The Pennsylvania State University, University Park, PA 16802, USA
[3] Institute of Bioorganic Chemistry, Polish Academy of Sciences, Z. Noskowskiego 12/14, 61-704 Poznan, Poland
[4] Present address: Cancer Research UK Nucleic Acid Structure Research Group, MSI/WTB Complex, University of Dundee, Dundee DD1 5EH, United Kingdom.
*Correspondence: pcb@chem.psu.edu
DOI 10.1016/j.chembiol.2006.11.004

SUMMARY

Recent studies indicate that RNA function can be enhanced by the incorporation of conformationally restricted nucleotides. Herein, we use 8-bromoguanosine, a nucleotide analog with an enforced *syn* conformation, to elucidate the catalytic relevance of ribozyme structures. We chose to study the lead-dependent ribozyme (leadzyme) because structural models derived from NMR, crystal, and computational (MC-Sym) studies differ in which of the three active site guanosines (G7, G9, or G24) have a *syn* glycosidic torsion angle. Kinetic assays were carried out on 8BrG variants at these three guanosine positions. These data indicate that an 8BrG24 leadzyme is hyperactive, while 8BrG7 and 8BrG9 leadzymes have reduced activity. These findings support the computational model of the leadzyme, rather than the NMR and crystal structures, as being the most relevant to phosphodiester bond cleavage.

INTRODUCTION

Recent advances in structure determination have led to dramatic increases in the numbers of high-resolution RNA structures, including RNA enzymes or ribozymes [1]. This has the potential to deepen insight into the chemistry of RNA enzymes. However, RNA has a tendency to adopt multiple conformations [2]; as such, the catalytic relevance of any RNA structure is best supported when biochemical and structural data are in agreement. Although this has been largely accomplished for some RNA enzymes [3, 4], structure-function discrepancies exist with regard to others [5, 6]. In the case of the hammerhead ribozyme, much of the discrepancy between structure and function has been lifted by recent crystallographic studies on an RNA construct with stronger native interactions [7]. This success story demonstrates that the choice of ribozyme construct plays a vital role in acquiring catalytically relevant data. Sterics can also play a major role in attaining a high fractional population of a catalytically relevant conformation [8]. Thus, it is possible that a conformationally restricted nucleotide, properly placed within an RNA enzyme, could accelerate catalysis.

Although global large-scale RNA misfolds can perturb RNA function significantly [2], less is known about the impact of local heterogeneity on function. Nucleotides have seven dihedral angles plus two sugar puckers, which lead to enormous conformational flexibility [9]. Of these angles, the glycosidic bond is of particular functional importance because it dictates how the nucleobase functional groups will be oriented. The typical *anti* conformation, in which the base is oriented away from the sugar, occurs in Watson-Crick helices. The rarer *syn* conformation, in which the base is oriented over the sugar, is found in UNCG tetraloops [10] and G quartets [11] and is often localized to functional regions of RNA molecules such as the catalytic centers of ribozymes [3, 12, 13] and the binding sites of aptamers (S.E. Krahe and P.C.B., unpublished data).

One approach for testing the functional relevance of a nucleobase orientation is to lock its conformation by using an analog with reduced conformational flexibility. The *syn* conformation is preferentially adopted by 8-bromoguanosine (8BrG) because the steric bulk of bromine disfavors its residence over the ribose sugar [14]. Indeed, 8BrG has been used to probe the *syn* conformation in G quartet [11] and UNCG [15, 16] motifs. Successful applications of 8BrG to these smaller systems suggested that this nucleotide analog might be useful for probing nucleobase orientations within a larger functional RNA, such as a ribozyme.

The leadzyme is an ~30 nt RNA that undergoes self-cleavage in the presence of Pb^{2+} ions [17] and has been implicated in lead toxicity in vivo [18]. Because of its small size and simple fold, the leadzyme has lent itself to a large number of mechanistic, thermodynamic, and structural studies [12]. However, despite 15 years of structure-function analyses, a consensus has yet to be reached on its

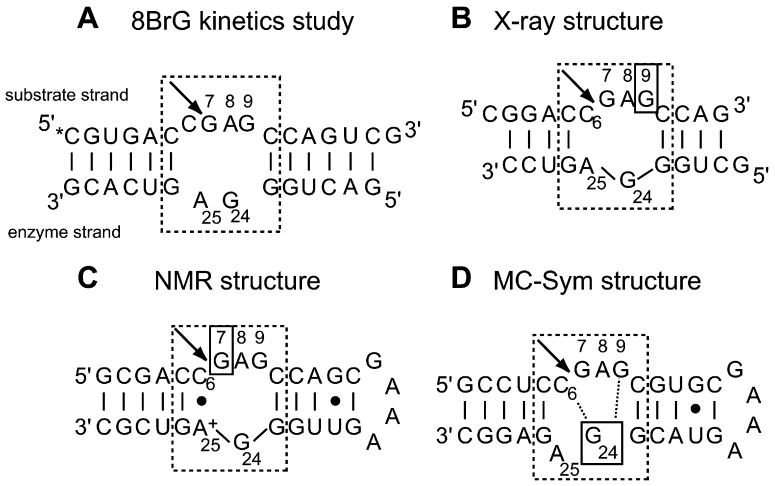

Figure 1. Secondary Structures of Leadzyme Constructs

(A–D) The numbering of active site bases is kept uniform and is done according to previous studies [23]. The active site loop is boxed, and the cleavage site is indicated with an arrow. (A) The two-piece leadzyme construct used in this study. The 5′ end of the substrate strand was radiolabeled with ^{32}P, designated with an asterisk. (B–D) Active site features of previously published leadzyme structures: (B) X-ray crystallography [21, 22], (C) NMR spectroscopy [23], and (D) MC-Sym calculations [24]. The *syn* base in each structure is boxed. Other features unique to each structure include an A$^+$•C wobble in the NMR structure and a base triple in the MC-Sym structure involving a G24-C6 reverse Watson-Crick pair and an asymmetric G24-G9 pairing to the Hoogsteen face of G24. This triple accounts for the stability of the *syn* conformation of G24 in the MC-Sym structure.

catalytically active conformation. In particular, while biochemical experiments have established G9 and G24 as being essential for catalysis [17, 19, 20], their orientation in three published structures differs greatly. Strikingly, a single *syn* G is located at three different positions within the active site (Figure 1): G9 in three of four "precatalytic" X-ray crystal structure conformations [21, 22], G7 in the averaged NMR structures [23], and G24 in an MC-Sym model [24]. The differences observed in these glycosidic torsion angles suggest that at least two of the structures are noncatalytic. Herein, we site specifically incorporate 8BrG at each of the three putative *syn* positions in the leadzyme and characterize the cleavage kinetics of each variant.

RESULTS AND DISCUSSION

Kinetics of 8BrG Leadzyme Variants

All kinetics experiments were carried out under single-turnover conditions. To facilitate site-specific incorporation of 8BrG by chemical synthesis, a two-piece leadzyme construct (Figure 1A) was used. This construct is a true enzyme in which the enzyme strand is unchanged during the reaction. In the presence of 300 μM Pb^{2+} (pH 7.0), the wild-type leadzyme reacted to over 80% completion, with a k_{obs} of 1.0 min^{-1} (Figure 2A). This rate constant is comparable to values obtained on a similar two-piece system (k_{obs} of 0.74 min^{-1} in 200 μM Pb^{2+}) [20].

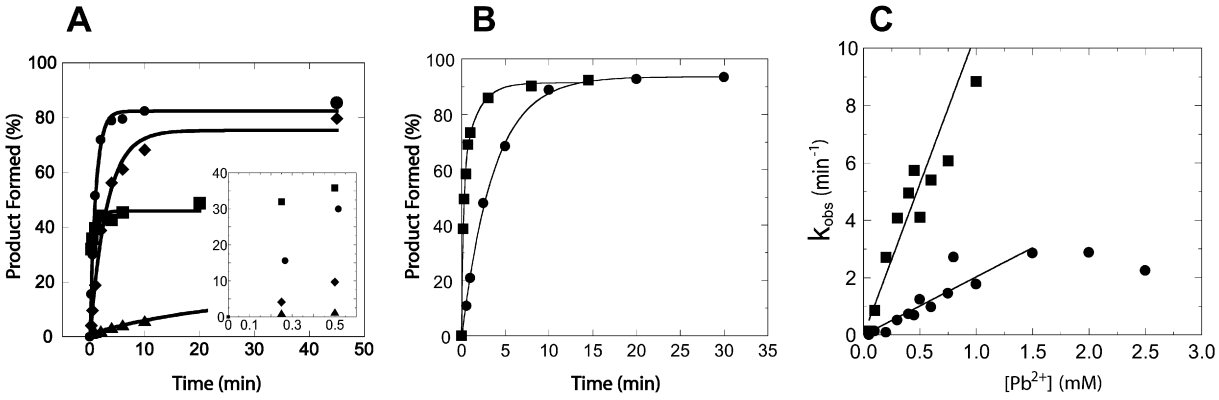

Figure 2. Effect of 8BrG Substitution at G7, G9, and G24 on Leadzyme Single-Turnover Kinetics

(A) Reaction profiles of 8BrG-modified leadzyme variants in 15 mM HEPES (pH 7.0) and 300 μM Pb^{2+}. Observed rate constants (k_{obs}) of 1.0, 0.33, 0.043, and 4.3 min^{-1} were determined for wild-type (circles), 8BrG7 (diamonds), 8BrG9 (triangles), and 8BrG24 (squares) variants, respectively. The inset shows time points out to the first 30 s.

(B) Reaction profiles of wild-type (circles) and 8BrG24 (squares) leadzymes in 10 mM MES (pH 6.0) and 300 μM Pb^{2+}. Observed rate constants (k_{obs}) of 0.33 and 4.5 min^{-1} were determined for wild-type and 8BrG24, respectively.

(C) Dependence of k_{obs} on Pb^{2+} concentration for wild-type (circles) and 8BrG24 (squares) leadzymes in 10 mM MES (pH 6.0). Slopes of 2.1 and 11 $mM^{-1}min^{-1}$ were found for wild-type and 8BrG24, respectively. Data beyond 1.5 mM Pb^{2+} were biphasic and thus were not included in the fit; the faster of the two rate constants is shown at 2.0 and 2.5 mM Pb^{2+} for visualization purposes only.

Table 1. Experimental Kinetics Data and Analysis of 8BrG-Substituted versus Wild-Type Leadzyme Reactivity

	$K_{dih\ 9}$[a]	$K_{dih\ 24}$[a]	Q[b]	Q_{rel}[c]	$k_{obs\ rel}$[d]; 300 μM Pb^{2+}, pH 7.0	$(k_{cat}/K_M)_{rel}$[d], pH 6.0
Wild-type	3	3	5.33	1	1 (1.0 min^{-1})	1 (2.1 $mM^{-1}min^{-1}$)
8BrG9	0.022	3	186	0.029	0.043 (0.043 min^{-1})	ND
8BrG24	3	0.022	1.4	3.9	4.3 (4.3 min^{-1})	5.2 (11 $mM^{-1}min^{-1}$)

[a] K_{dih} is the nucleobase preference for the *anti* conformation. It is the ratio of the concentrations between the *anti* and *syn* conformations. These values are assigned on the basis of experiments conducted on 8BrG-substituted oligonucleotides, as described in "Effect of 8BrG Substitutions on Ribozyme Activity." Errors in the numbers 3 and 0.022 in K_{dih} are 10%–20% each, based on previously published error values [15, 16]. When propagated, this leads to conservative estimations of overall errors for the partition function of 6%, 18%, and 30% for 8BrG24, wild-type, and 8BrG9, respectively. These errors are small compared to the relative kinetic values in the last two columns, which show 5- to 23-fold effects. Errors in the kinetics constants in the last two columns come from the statistics of nonlinear curve fitting and were typically under 10% error.
[b] Q is the sum of the weighted population of the nonnative conformations and is calculated according to Equation 6.
[c] Q_{rel} values are normalized inversely with respect to the wild-type.
[d] In order to make comparisons between 8BrG and wild-type leadzyme, observed rates (in parentheses) are normalized with respect to the wild-type data to give $k_{obs\ rel}$ and $(k_{cat}/K_M)_{rel}$ values.

When 8BrG was substituted at position 7, there was a 3-fold decrease in k_{obs} to 0.33 min^{-1} at 300 μM Pb^{2+} (pH 7.0) (Figure 2A; Table 1). This modest effect suggests that G7 has a slight preference for adopting an *anti* conformation, consistent with the crystal and MC-Sym structures. Alternatively, it is possible that position 7 prefers the *syn* conformation but that the bromine interferes with folding. However, this scenario seems unlikely, as there is ample room to accommodate bromine at G7 in the NMR structure (not shown). Moreover, the 8BrG kinetics results are consistent with in vitro selection experiments [19, 20], which showed that the identity of the nucleotide at G7 is not critical for activity.

When 8BrG was substituted at position 9, there was a 23-fold decrease in k_{obs} to 0.043 min^{-1} at 300 μM Pb^{2+} (pH 7.0) (Figure 2A). This large inhibitory effect suggests that G9 has a strong preference for an *anti* conformation. These kinetics results are consistent with both the NMR and MC-Sym structures wherein G9 is *anti*, although G9 is *anti* for different reasons (see below). In the precatalytic crystal structure, G9 is *syn*, suggesting that this position does not represent a catalytic conformation of the leadzyme.

When 8BrG was substituted at position G24, there was a 4-fold *increase* in k_{obs} to 4.3 min^{-1} at 300 μM Pb^{2+} (pH 7.0) (Figure 2A and inset), with the actual rate enhancement varying from 3- to 30-fold depending on lead concentration and pH (see "Ribozyme Kinetics" in Experimental Procedures). The observed rate acceleration strongly supports G24 preferring a *syn* glycosidic torsion angle for catalysis. One possible explanation for the rate enhancement is that the 8Br substitution preorganizes the active site into a catalytic conformation (see "Effect of 8BrG Substitutions on Ribozyme Activity" for models and analyses). Remarkably, the MC-Sym model is the only structure that proposes a *syn* conformation for G24 [24]. In this structure, the *syn* conformation of G24 is stabilized by a triple interaction involving two other essential nucleotides, C6 and G9 (see Results and Discussion and Figure 4D).

The Leadzyme 8BrG24 Variant Is Hyperactive

Enhancement of leadzyme function by the 8BrG24 substitution was tested by additional kinetics analyses, including comparing the dependence of k_{obs} on Pb^{2+} concentration for wild-type and 8BrG24 ribozymes. The pH was lowered to 6.0 for these experiments to slow the rate of the reaction [19] (Figure 2) and to drive it to completion (at higher pH, lead hydroxide and polyhydroxides can interfere with reaction analysis [19]). Between 50 and 1500 μM Pb^{2+} concentrations, reaction profiles for wild-type and 8BrG24 leadzymes were single exponential and proceeded to 90% completion (Figure 2B). Moreover, over this range of Pb^{2+} concentration, plots of k_{obs} versus Pb^{2+} concentration for wild-type and 8BrG leadzymes were linear, with y intercepts of zero (Figure 2C). The slopes of the two lines were 2.1 and 11 $mM^{-1}min^{-1}$ for wild-type and 8BrG24, respectively, consistent with ~5-fold catalytic stimulation by a *syn* G24. Slopes of k_{obs} versus substrate concentration are generally interpretable in terms of a k_{cat}/K_m parameter (see next section). In an effort to determine whether the observed difference in the slopes was due to effects on k_{cat}, K_m, or both, we examined the effect of higher Pb^{2+} concentrations on k_{obs}. Unfortunately, reaction profiles for 8BrG24 and wild-type leadzymes were biphasic at Pb^{2+} concentrations above 1.2 mM. The absence of simple saturation behavior precluded a determination of individual kinetic constants (see Experimental Procedures); nevertheless, the linear dependence of k_{obs} on Pb^{2+} concentration at subsaturating concentrations of Pb^{2+} clearly showed rate enhancement in the presence of G24 with an enforced *syn* conformation. A minimal kinetic model that is consistent with the data is presented in the following section (see Figure 3).

Effect of 8BrG Substitutions on Ribozyme Activity

Figure 3A presents a simple kinetic model that accounts for the effect of a conformational pre-equilibrium on the observed rates of ribozyme cleavage. In all cases, even

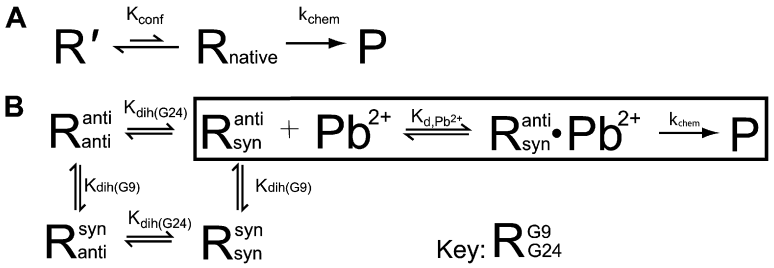

Figure 3. Kinetic Models for Ribozyme Cleavage

(A and B) Various conformations of the ribozyme are depicted as "R," and the product of the reaction is depicted as "P." (A) A general model for ribozyme cleavage. R_{native} represents the functional fold that can undergo catalysis via k_{chem}, whereas R′ is a catalytically inactive fold (which may be stable relative to R_{native}) that needs to be resolved. (B) A model specific for the leadzyme in which the native state binds Pb^{2+} and proceeds to product formation (boxed region). In this scheme, the ribozyme, R, exists in four possible conformations with differing torsion angles at G9 and G24. The torsion angles for G9 and G24 are denoted in superscript and subscript respectively (R^{G9}_{G24}). On the basis of the 8BrG kinetics data, only one of the four conformations, R^{anti}_{syn}, is poised to bind Pb^{2+} and form products. Inactive states can adopt the reactive state, R^{anti}_{syn}, by rotating a torsion angle to the correct conformation (K_{dih}).

though a two-piece ribozyme is used, only a single R state is shown; this is because saturating single-turnover conditions were used, as described in the Experimental Procedures. The ribozyme is assumed to have two conformations, R_{native} and R′, which represent catalytically active and inactive states, respectively. These states are related by a conformational equilibrium constant, $K_{conf} = [R']/[R_{native}]$, in which the native ribozyme is chosen as the reference state; accordingly, large values of K_{conf} reflect decreased reactivity. The intrinsic rate constant for chemistry is k_{chem}, which can be attained when the ribozyme is natively folded. In this analysis, R_{native} is in rapid equilibrium with R′, which is reasonable if R_{native} is more likely to decompose than to form products; indeed, the conformational equilibrium constants considered for 8BrG substitution involve simple rotations about the glycosidic bond, which are likely to be rapid, and observation of single-exponential behavior at all Pb^{2+} concentrations further supports this model. According to the model in Figure 3A, the observed rate constant, k_{obs}, is the product of the rate-limiting step for the reaction, k_{chem}, and the fraction of molecules having the native tertiary fold, f_{native} [25]:

$$k_{obs} = k_{chem} \times f_{native}. \quad (1)$$

This leads to a simple functional form

$$k_{obs} = k_{chem}/(1 + K_{conf}), \quad (2)$$

where K_{conf} is the ratio between nonnative and native state concentrations, as defined earlier. Thus, as the nonnative ribozyme population grows, K_{conf} increases, and, as a consequence, k_{obs} decreases.

Figure 3B presents a more complex version of the kinetic model in Figure 3A, which is appropriate for the leadzyme. This model provides explicit consideration of the glycosidic torsion angles of G9 and G24. (G7 is not considered in this model because its conformation has a smaller effect on kinetics; moreover, the identity of the nucleotide at this position is relatively unimportant according to in vitro experiments [19]—A, G, and U are tolerated equally, and C likely leads to a misfold—and G7 is positioned away from the active site in the MC-Sym model [24].) In addition, the intrinsic rate constant for chemistry, k_{chem}, is left unchanged by the bromine substitution, which is reasonable given that the 8 position of G24 is pointed into solution in the MC-Sym model. On the basis of the activity studies with 8BrG-substituted leadzymes, the native state is denoted as $R^{anti}_{syn} \bullet Pb^{2+}$, in which G9 is *anti*, G24 is *syn*, and Pb^{2+} is bound. Only ribozyme molecules that are natively folded (where both G9 is *anti* and G24 is *syn*, or R^{anti}_{syn}) are considered to be poised to bind a Pb^{2+} ion in a catalytically active fashion, with an intrinsic dissociation constant, $K_{d,Pb2+}$. According to this model, ribozyme molecules depicted in the three other states (where G9, G24, or both have nonnative glycosidic conformations) do not bind a Pb^{2+} ion in a catalytically active fashion. A consequence of these nonnative conformations is that $K_{d,obs}$ for Pb^{2+} binding increases (Equation 5), where nonnative states are related to the native, cleavage-ready state by conformational equilibrium constants, K_{dih}, defined below.

One notable feature of the model depicted in Figure 3B is that the intrinsic constants $K_{d,Pb2+}$ and k_{chem} (boxed region) do not change in value as different 8BrG-substituted ribozymes are considered. As such, substitution of 8BrG changes the relative population of the nonnative Pb^{2+}-free states, but not of the native R^{anti}_{syn} to $R^{anti}_{syn} \bullet Pb^{2+}$ states. This model is consistent with the notion that RNA can exist in many states, one of which can be "captured" by another species to go on to serve a functional role [26].

The presence of nonnative glycosidic conformations at G9 and G24 can be described by expanding the relationship in Equation 2 to give

$$k_{obs} = \frac{k_{chem}[Pb^{2+}]}{K_{d,intr}\left(1 + K_{dih24} + \frac{1}{K_{dih9}} + \frac{K_{dih24}}{K_{dih9}}\right) + [Pb^{2+}]}, \quad (3)$$

where R^{anti}_{syn} was chosen as the reference state, and the conformational equilibrium constant, $K_{dih\ i}$, is the ratio of the concentrations of the *anti* and *syn* conformers of the G9 or G24 nucleobase. Equation 4 is similar to a general hyperbolic kinetic equation:

$$k_{obs} = \frac{k_{chem}[Pb^{2+}]}{K_{d,obs} + [Pb^{2+}]}. \quad (4)$$

From Equation 4, we define an observed binding constant, $K_{d,obs}$, for Pb^{2+} as

$$K_{d,obs} = K_{d,intr}Q, \quad (5)$$

where

$$Q = 1 + K_{dih24} + \frac{1}{K_{dih9}} + \frac{K_{dih24}}{K_{dih9}}. \quad (6)$$

The Q value in Equation 6 is a partition function that enumerates the conformational heterogeneity of the Pb^{2+}-free ribozyme population. Quantitatively, a low Q value would represent a higher fractional population of the reference state R^{anti}_{syn}, whereas a higher Q value would represent occupancy of nonnative Pb^{2+}-free states. The larger Q value would result in a larger $K_{d,obs}$, as shown by the proportionality in Equation 5.

As stated earlier, kinetic behavior was multiexponential at high Pb^{2+} concentrations, which precluded attainment of saturation conditions and, therefore, $K_{d,obs}$ values. As such, most of the analyses are expressed in terms of subsaturating Pb^{2+} concentrations. According to Equation 4, this is equivalent to $k_{chem}/K_{d,obs}$, or k_{cat}/K_m, behavior. k_{cat}/K_m is often referred to as the "specificity constant" [27], and, in this case, ratios of k_{cat}/K_m for different leadzyme variants describe the reactivity of one variant relative to another under otherwise identical conditions of lead concentration (Table 1).

In order to assess the effect of nonnative glycosidic torsion angles on activity, we considered appropriate values for K_{dih} from experiments. These values are chosen on the basis of whether the ribozyme is unsubstituted or 8BrG substituted at the position of interest. K_{dih} for an unmodified guanosine is assigned a value of 3, which is derived from an observed 4-fold acceleration of folding rate upon substitution of 8BrG into position 4 of a UUCG tetraloop [16]; the UUCG tetraloop naturally has a *syn* guanosine at position 4 of the loop, and, according to Equation 2, the rate of folding of the native (unsubstituted) loop is decreased by the observed 4-fold effect if an *anti* preference of 3 is used for K_{conf} (=K_{dih}). The value of K_{dih} for an 8Br-modified guanosine was determined from experimentation as well. K_{dih} for 8BrG is assigned an *anti* preference of 0.022. This value is assigned on the basis of the observation that substitution of 8BrG into a GC base pair that is in an internal helical position leads to a $\Delta\Delta G^{\circ}_{37}$ destabilization of +2.36 kcal/mol [15].

Next, these values for K_{dih} were used to predict the effect of having an 8BrG substitution at G9 and G24, and were compared to the experimentally determined kinetics results. For the wild-type ribozyme, a K_{dih} value of 3 was used for G9 and G24, which gives a Q_{wt} of 5.33 (Table 1). For 8BrG9, K_{dih} values of 0.022 and 3 were used for G9 and G24, respectively, which provides a Q_{G9} of 186. In order to make direct comparisons between 8BrG-substituted and unsubstituted leadzymes, Q values were normalized with respect to wild-type, to give Q_{rel}. For the 8BrG9 ribozyme, the Q_{G9rel} value is 0.029, which is in good agreement with the experimental $k_{obs\ rel}$ value of 0.043 obtained at pH 7.0.

Finally, we consider the 8BrG24-substituted leadzyme. Here, K_{dih} values of 3 and 0.022 were used for G9 and G24, respectively, which provides a Q_{G24} of 1.4 and a Q_{G24rel} of 3.9 (Table 1). Note that the difference in magnitude is much greater between Q_{G24} and Q_{G9} than between Q_{G24} and Q_{wt} (1.4 versus 186, and 1.4 versus 5.3, respectively). These effects arise because a steric block is more effective at disfavoring a native state than it is at favoring a native state. The Q_{G24rel} value of 3.9 is in good agreement with the experimental $k_{obs\ rel}$ value of 4.3 at pH 7.0, and with the $(k_{cat}/K_M)_{rel}$ value of 5.2 at pH 6.0. Agreement between Q_{rel} values and kinetic constants for the leadzyme variants suggests that the kinetic model in Figure 3B provides a good description of the behavior of the leadzyme.

8BrG Kinetics Reveal Nucleobase Orientations Relevant to Catalysis

Substitution of the leadzyme active site guanosines with 8BrG led to as much as 30-fold stimulation at position 24 (Figure 2C and "Ribozyme Kinetics" in Experimental Procedures) and modest (3-fold) to substantial (23-fold) inhibition at positions 7 and 9, respectively (Figure 2A). This set of data is most consistent with the MC-Sym structure having catalytic relevance. Moreover, it is anticipated that a *syn* G24 would be incongruent with the NMR [23] and crystallographic structures [22], as G24 is *anti* in these structures and is tightly packed (Figure 4C). Absence of *direct* catalytic relevance of the NMR and X-ray structures is not surprising given that A25 of the A^{+}•C wobble present in the NMR structures can be deleted and activity increases [20], and that much of the active site of the X-ray structure is involved in crystal-crystal interactions [21, 22]. The results here suggest these structures must undergo major rearrangements involving glycosidic bond rotations to attain the catalytic conformation. Nevertheless, it remains possible that the NMR and crystal structures represent populated ground states on the reaction or folding pathway. Indeed, NMR studies have shown that leadzyme structures are dynamic, suggestive of motions that may lead to a near-active conformation [28, 29]. This flexibility is also supported by the first set of crystallographic structures on the leadzyme, in which crystallographically independent structures revealed large differences in positioning of the backbone [21].

A comparison of the backbones of the three structures is provided in Figure 4. NMR and crystallography structures are similar in overall shape (Figure 4A). In contrast, the MC-Sym model has a drastically different backbone conformation near the active site (Figure 4B). Figure 4D shows that the triple mediated by *syn* G24 is at the core of the active site. Substantiation of the *syn* conformation of G24 by the experiments herein strongly supports this major conformational restraint, although the authenticity of other structural interactions in the MC-Sym model has to await additional high-resolution experimental structures. Given the propensity for RNA molecules to have *syn* bases in their functional domains (S.E. Krahe and P.C.B., unpublished data), it is possible that conformationally

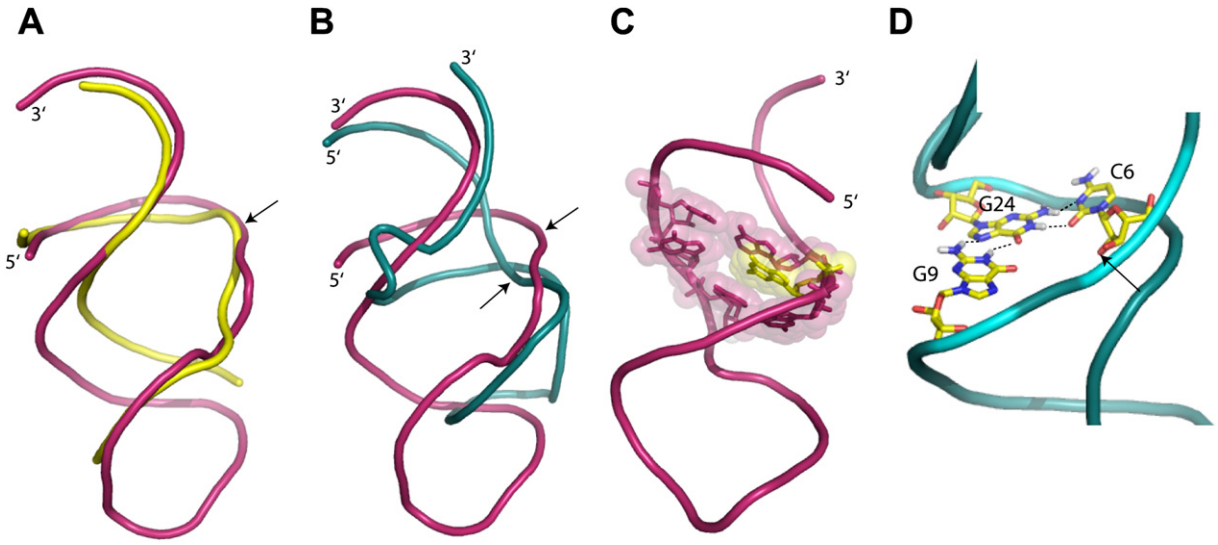

Figure 4. Backbone Superposition for the Three Leadzyme Structures

(A–D) The site of self-cleavage is depicted with an arrow. (A) Overlay of NMR (magenta) and X-ray crystallographic (yellow) structures. The site of self-cleavage in these two structures is virtually identical; thus, only a single arrow is depicted. These two structures have similar overall geometries. (B) Overlay of NMR (magenta) and MC-Sym (teal) structures. The site of self-cleavage is shown separately for each structure. These two structures have quite different overall geometries. (C) NMR structure with active site nucleobases rendered in CPK. G24 (yellow) adopts an *anti* conformation in the NMR structure and engages in base-stacking interactions. Changing the conformation of G24 to *syn* would likely disrupt this active site. (D) Expanded view of the MC-sym structure displaying the G24-C6-G9 base triple interactions (in stick representation) that stabilize the *syn* conformation of G24. The hydrogen bonding depicted includes the reverse Watson-Crick pair between G24 and C6 and the asymmetric pairing between G24 and G9. The arrow points to the nucleophilic 2′-hydroxyl of C6. The view is rotated 180° with respect to (B) to emphasize the importance of the base triple in determining the structural integrity of the active site. PDB files used in this figure are 2ldz, 1nuj (strands C and D in the "precatalytic" conformer pdb file), and http://www-lbit.iro.umontreal.ca/structures/leadzyme.pdb for the NMR [23], X-ray [22], and MC-sym [24] structures, respectively. Superposition of the structures was performed using the program O [31], and figures were prepared with PyMOL [32].

restricted nucleotides will provide a generally useful tool for functional and structural studies on large RNAs.

SIGNIFICANCE

Numerous high-resolution structures of catalytic RNAs have appeared in recent years, and these have the potential to provide deep insight into function. However, in several small ribozymes, there is discrepancy between structural and functional data. Thus, new approaches that can address structure-function discrepancies in ribozymes are needed. The lead-dependent ribozyme is a case wherein structures obtained from NMR, X-ray crystallography, and computational modeling reveal structural differences at catalytically essential nucleobases within the enzyme active site. In particular, a unique guanosine is found in the *syn* conformation within the active site of each of three leadzyme structures. In this study, we used 8BrG to decipher the correct orientation of guanosine glycosidic torsion angles in the leadzyme in order to determine which, if any, of these structures might represent the cleavage-active state. In contrast to a standard guanosine nucleobase, 8BrG is a conformationally restricted nucleotide that preferentially adopts the *syn* glycosidic torsion angle. Upon substitution of 8BrG at each of the three putative *syn* positions in the leadzyme, we find that 8BrG substitution in the position of the MC-Sym *syn* base (position 24) leads to hyperactivity, with as much as a 30-fold increase in rate, whereas substitution in the position of X-ray or NMR *syn* bases leads to substantial rate decreases. Moreover, the latter two models should not have been tolerant of a *syn* base at position 24 due to packing. Collectively, these data strongly support the functional relevance of the catalytic core represented in the MC-Sym computational model rather than the X-ray or NMR structures. Results from this study show that conformationally restricted nucleotides such as 8BrG can be useful tools for judging the catalytic relevance of RNA structures, as well as providing a potential means for coaxing RNAs to crystallize in functionally relevant states to aid in determination of experimental structures.

EXPERIMENTAL PROCEDURES

Leadzyme Design and Preparation

A two-piece leadzyme was adapted from a stable, fast-reacting leadzyme used in previous biochemical studies [20] and consists of a 4 × 2 purine-rich internal loop flanked by 6 base pairs on both sides. In addition, a dangling guanosine was appended to the 3′ end of the substrate strand to increase the stability of the enzyme-substrate complex by an additional 1.7 kcal/mol [30]. Wild-type substrate and enzyme RNA oligonucleotides were purchased from Dharmacon, Inc. and were deprotected and desalted according to the manufacturer's

protocol. 8BrG was synthesized as a phosphoramidite and incorporated into RNA oligonucleotides as described elsewhere [15, 16]. After desalting and purification, the molecular weight of each modified oligonucleotide was confirmed by electrospray-mass spectrometry (Huck Institutes Mass Spectrometry Core Facility, Penn State University). For kinetics experiments, leadzyme substrate oligonucleotides were 5′ end-labeled with [γ-^{32}P]ATP by T4 polynucleotide kinase (New England Biolabs), purified by a G-25 Sephadex spin column (Roche), and stored at a concentration of ~0.5 μM in 1× TE. Solutions of $Pb(OAc)_2$ were freshly prepared as 10× stock solutions for kinetic studies.

Ribozyme Kinetics

RNA self-cleavage reactions were conducted under single-turnover conditions with ~5 nM of 5′ end-labeled substrate, 10 μM enzyme in 10–15 mM buffer (MES [pH 6.0]; HEPES [pH 7.0]), and 0.05–4 mM $Pb(OAc)_2$. Controls with up to 10,000-fold excess enzyme strand gave similar rates, consistent with saturation in single-turnover experiments. The RNA was renatured by using conditions previously described for a two-piece leadzyme system: 70°C for 90 s and then flash cooling on ice [20]. This mixture was preincubated at 25°C for 10 min, and the reaction was initiated with the addition of a 10× solution of $Pb(OAc)_2$. For each time point, 3 μl aliquots were removed, quenched in 4 μl 20 mM EDTA formamide loading buffer, and immediately stored on powdered dry ice. Reaction mixtures were fractionated on a denaturing 10% polyacrylamide gel. RNA precursor and product bands were analyzed with a PhosphorImager scanner and were quantitated by using ImageQuant software (Molecular Dynamics).

Single-turnover kinetics data were initially collected at pH 7.0 and 25°C. A Pb^{2+} titration of the wild-type leadzyme provided a bell-shaped dependence, with 300 μM Pb^{2+} providing the fastest reactivity, in accord with previous studies [19, 20]. However, certain reactions proceeded to only ~50% completion and proved too fast for accurate measurement by hand mixing. In addition, at higher Pb^{2+} and pH conditions, the RNA is susceptible to nonspecific degradation, and the free concentration of Pb^{2+} becomes uncertain due to polyhydroxide formation [19, 20]. For these two reasons, the pH was lowered to 6.0 for more detailed kinetic analyses on wild-type and 8BrG24 ribozymes. Reactions under these conditions could be determined accurately by hand mixing and were found to proceed to completion up to much higher Pb^{2+} concentrations than at pH 7.0. Most of the data at pH 6.0 were well fit by a single-exponential equation, $f = A + Be^{-k_{obs}t}$, where f is the fraction reacted and k_{obs} is the observed rate constant for self-cleavage; reactions were single exponential with no burst (i.e., $B \approx -A$) and proceeded to greater than 80% completion at a low Pb^{2+} concentration. At a low Pb^{2+} concentration, 8BrG24-modified ribozymes reacted as much as 30-fold faster than wild-type: at 200 μM Pb^{2+}, rate constants were 2.7 min^{-1} and 0.09 min^{-1} for 8BrG24 and wild-type ribozyme, respectively (Figure 2C). However, at pH 6.0, Pb^{2+} concentrations above 1.5 mM led to double-exponential kinetics for both wild-type and 8BrG24 variants. Thus, the data were analyzed according to a k_{cat}/K_m formalism with 1.5 mM and lower data.

ACKNOWLEDGMENTS

We would like to acknowledge the following agencies for generous support: American Chemical Society-Petroleum Research Fund and National Science Foundation grant MCB-0527102 (P.C.B.), National Institutes of Health grant #1R03TW1068 (R.K. and D.H. Turner), and the Natural Sciences and Engineering Research Council of Canada for a post-graduate scholarship (R.Y.). We also would like to thank Katsu Murakami for assistance in preparing Figure 4, and Steve Benkovic, Barbara Golden, Sharon Hammes-Schiffer, and Doug Turner for suggestions on the manuscript. We dedicate this paper to Doug Turner on the occasion of his 60th birthday.

Received: September 1, 2006
Revised: October 26, 2006
Accepted: November 6, 2006
Published: January 26, 2007

REFERENCES

1. Holbrook, S.R. (2005). RNA structure: the long and the short of it. Curr. Opin. Struct. Biol. *15*, 302–308.
2. Treiber, D.K., and Williamson, J.R. (2001). Beyond kinetic traps in RNA folding. Curr. Opin. Struct. Biol. *11*, 309–314.
3. Rupert, P.B., Massey, A.P., Sigurdsson, S.T., and Ferre-D'Amare, A.R. (2002). Transition state stabilization by a catalytic RNA. Science *298*, 1421–1424.
4. Stahley, M.R., and Strobel, S.A. (2005). Structural evidence for a two-metal-ion mechanism of group I intron splicing. Science *309*, 1587–1590.
5. Blount, K.F., and Uhlenbeck, O.C. (2005). The structure-function dilemma of the hammerhead ribozyme. Annu. Rev. Biophys. Biomol. Struct. *34*, 415–440.
6. Bevilacqua, P.C., and Yajima, R. (2006). Nucleobase catalysis in ribozyme mechanism. Curr. Opin. Chem. Biol. *10*, 455–464.
7. Martick, M., and Scott, W.G. (2006). Tertiary contacts distant from the active site prime a ribozyme for catalysis. Cell *126*, 309–320.
8. Benkovic, S.J., and Hammes-Schiffer, S. (2003). A perspective on enzyme catalysis. Science *301*, 1196–1202.
9. Bloomfield, V.A., Crothers, D.M., and Tinoco, I., Jr. (2000). Nucleic Acids: Structures, Properties, and Functions (Sausalito, CA: University Science Books).
10. Cheong, C., Varani, G., and Tinoco, I., Jr. (1990). Solution structure of an unusually stable RNA hairpin, 5′GGAC(UUCG)GUCC. Nature *346*, 680–682.
11. Dias, E., Battiste, J.L., and Williamson, J.R. (1994). Chemical probe for glycosidic conformation in telomeric DNAs. J. Am. Chem. Soc. *116*, 4479–4480.
12. David, L., Lambert, D., Gendron, P., and Major, F. (2001). Leadzyme. Methods Enzymol. *341*, 518–540.
13. Sigel, R.K., Sashital, D.G., Abramovitz, D.L., Palmer, A.G., Butcher, S.E., and Pyle, A.M. (2004). Solution structure of domain 5 of a group II intron ribozyme reveals a new RNA motif. Nat. Struct. Mol. Biol. *11*, 187–192.
14. Tavale, S.S., and Sobell, H.M. (1970). Crystal and molecular structure of 8-bromoguanosine and 8-bromoadenosine, two purine nucleosides in the syn conformation. J. Mol. Biol. *48*, 109–123.
15. Proctor, D.J., Kierzek, E., Kierzek, R., and Bevilacqua, P.C. (2003). Restricting the conformational heterogeneity of RNA by specific incorporation of 8-bromoguanosine. J. Am. Chem. Soc. *125*, 2390–2391.
16. Proctor, D.J., Ma, H., Kierzek, E., Kierzek, R., Gruebele, M., and Bevilacqua, P.C. (2004). Folding thermodynamics and kinetics of YNMG RNA hairpins: specific incorporation of 8-bromoguanosine leads to stabilization by enhancement of the folding rate. Biochemistry *43*, 14004–14014.
17. Pan, T., and Uhlenbeck, O.C. (1992). A small metalloribozyme with a two-step mechanism. Nature *358*, 560–563.
18. Barciszewska, M.Z., Szymanski, M., Wyszko, E., Pas, J., Rychlewski, L., and Barciszewski, J. (2005). Lead toxicity through the leadzyme. Mutat. Res. *589*, 103–110.
19. Pan, T., Dichtl, B., and Uhlenbeck, O. (1994). Properties of an in vitro selected Pb^{2+} cleavage motif. Biochemistry *33*, 9561–9565.

20. Chartrand, P., Usman, N., and Cedergren, R. (1997). Effect of structural modifications on the activity of the leadzyme. Biochemistry *36*, 3145–3150.

21. Wedekind, J.E., and McKay, D.B. (1999). Crystal structure of a lead-dependent ribozyme revealing metal binding sites relevant to catalysis. Nat. Struct. Biol. *6*, 261–268.

22. Wedekind, J.E., and McKay, D.B. (2003). Crystal structure of the leadzyme at 1.8 Å resolution: metal ion binding and the implications for catalytic mechanism and allo site ion regulation. Biochemistry *42*, 9554–9563.

23. Hoogstraten, C.G., Legault, P., and Pardi, A. (1998). NMR solution structure of the lead-dependent ribozyme: evidence for dynamics in RNA catalysis. J. Mol. Biol. *284*, 337–350.

24. Lemieux, S., Chartrand, P., Cedergren, R., and Major, F. (1998). Modeling active RNA structures using the intersection of conformational space: application to the lead-activated ribozyme. RNA *4*, 739–749.

25. Bevilacqua, P.C., Brown, T.S., Chadalavada, D., Parente, A.D., and Yajima, R. (2003). Kinetic Analysis of Ribozyme Cleavage (Oxford: Oxford University Press).

26. Weeks, K.M., and Cech, T.R. (1996). Assembly of a ribonucleoprotein catalyst by tertiary structure capture. Science *271*, 345–348.

27. Fersht, A. (1985). Enzyme Structure and Mechanism, Second Edition (New York: Freeman).

28. Legault, P., Hoogstraten, C.G., Metlitzky, E., and Pardi, A. (1998). Order, dynamics and metal-binding in the lead-dependent ribozyme. J. Mol. Biol. *284*, 325–335.

29. Hoogstraten, C.G., Wank, J.R., and Pardi, A. (2000). Active site dynamics in the lead-dependent ribozyme. Biochemistry *39*, 9951–9958.

30. Turner, D.H., Sugimoto, N., and Freier, S.M. (1988). RNA structure prediction. Annu. Rev. Biophys. Biophys. Chem. *17*, 167–192.

31. Jones, T.A., Zou, J.Y., Cowan, S.W., and Kjeldgaard, M. (1991). Improved methods for building protein models in electron-density maps and the location of errors in these models. Acta Crystallogr. A *47*, 110–119.

32. DeLano, W.L. (2002). The PyMOL Molecular Graphics System (San Carlos, CA: DeLano Scientific).

